HHS Public Access

Author manuscript

Liver Int. Author manuscript; available in PMC 2022 October 01.

Published in final edited form as:

Liver Int. 2022 April ; 42(4): 829–841. doi:10.1111/liv.15182.

Anti-CD47 antibody treatment attenuates liver inflammation and fibrosis in experimental non-alcoholic steatohepatitis models

Taesik Gwag[1], **Eric Ma**[1], **Changcheng Zhou**[2], **Shuxia Wang**[1,*]

[1]Department of Pharmacology and Nutritional Sciences, University of Kentucky, Lexington, KY 40536, and Lexington VA Medical Center, Lexington KY 40502.

[2]Division of Biomedical Sciences, School of Medicine, University of California, Riverside, CA 92521

Abstract

Background and Aims: With the epidemic burden of obesity and metabolic diseases, nonalcoholic fatty liver disease (NAFLD) including steatohepatitis (NASH) has become the most common chronic liver disease in the western world. NASH may progress to cirrhosis and hepatocellular carcinoma. Currently no treatment is available for NASH. Therefore, finding a therapy for NAFLD/NASH is in urgent need. Previously we have demonstrated that mice lacking CD47 or its ligand thrombospondin1 (TSP1) are protected from obesity-associated NALFD. This suggests that CD47 blockade might be a novel treatment for obesity-associated metabolic disease. Thus, in this study, the therapeutic potential of an anti-CD47 antibody in NAFLD progression was determined.

Methods: Both diet-induced NASH mouse model and human NASH organoid model were utilized in this study. NASH was induced in mice by feeding with diet enriched with fat, fructose and cholesterol (AMLN diet) for 20 weeks and then treated with anti-CD47 antibody or control IgG for 4 weeks. Body weight, body composition and liver phenotype were analyzed.

Results: We found that anti-CD47 antibody treatment did not affect mice body weight, fat mass, or liver steatosis. However, liver immune cell infiltration, inflammation and fibrosis were significantly reduced by anti-CD47 antibody treatment. *In vitro* data further showed that CD47 blockade prevented hepatic stellate cell activation and NASH progression in a human NASH organoid model.

Conclusion: Collectively, these data suggest that anti-CD47 antibody might be a new therapeutic option for obesity-associated NASH and liver fibrosis.

*To whom correspondence should be addressed: Shuxia Wang, MD, PhD, Department of Pharmacology and Nutritional Sciences, University of Kentucky, Wethington Bldg. Room 583, 900 S. Limestone Street, Lexington, KY 40536. Tel: 859-218-1367, Fax: 859-257-3646, swang7@uky.edu.

Author Contributions:

Designed research: SW. Performed experiments: TG, EM. Analysis and interpretation of the data: all. Wrote manuscript: TG, SW. Approved final version of the manuscript: all.

Conflict of interest disclosure:

No conflicts of interest, financial or otherwise, are declared by the authors.

Ethics approval statement:

All the experiments involving mice conformed to the National Institutes of Health Guide for the Care and Use of Laboratory Animals and were approved by the University of Kentucky Institutional Animal Care and Use Committee.

Lay summary:

Obesity-associated nonalcoholic fatty liver disease (NAFLD) is a most common chronic liver disease in the Western world and may progress to liver cirrhosis and cancer. Currently no treatment is available for this disease. The present study tests a novel therapeutic potential of an anti-CD47 antibody in NAFLD progression by utilization of preclinical NAFLD models and provide strong evidence that this antibody may serve as a new treatment option for NAFLD.

Keywords

NAFLD; NASH; CD47; obesity; AMLN diet; organoid

Introduction

Due to the epidemic of obesity and diabetes, NAFLD has become the most common liver disease around the world [1]. NAFLD ranges from nonalcoholic fatty liver (NAFL) to nonalcoholic steatohepatitis (NASH), characterized by NAFL, hepatocellular ballooning and lobular inflammation with varying degrees of fibrosis, and may progress to cirrhosis and hepatocellular carcinoma. Currently, there is no NAFLD therapy. Lifestyle interventions like diet and exercise are one of the only treatments available to those suffered from NAFLD. However, they do not achieve satisfactory results [2]. Therefore, an effective alternative strategy is urgently needed.

CD47 is a transmembrane glycoprotein that expresses universally on the surface of various cell types. It plays a role in immunity, self-recognition, stress response, cell survival et al [3-7]. In addition, our recent studies reveled a novel role of CD47 or its ligand-thrombospondin1 (TSP1) in the development of obesity and its associated metabolic diseases [8,9]. We demonstrated that CD47 deficiency protected mice from diet-induced obesity and obesity-associated fatty liver diseases [9]. TSP1 deficiency or particularly macrophage specific TSP1 deficiency reduced obesity-associated liver injury, accompanied by reduced liver inflammation and fibrosis [8]. These studies suggest that blocking CD47 singling such as using anti-CD47 antibody might be a novel therapeutic option for obesity-associated NAFLD/NASH. Anti-CD47 antibody has been entered into clinical trial for various of cancer types. However, its application in NAFLD/NASH has never been explored.

In the current study, the therapeutic effect of anti-CD47 antibody on NASH development/progression was tested in both diet-induced NASH mouse model and 3D human NASH organoid model. In established NASH mouse model, anti-CD47 antibody treatment prevented NASH progression *in vivo* by inducing partial resolution of liver inflammation and fibrosis although steatosis was not improved. In addition, this protective effect was also seen in human NASH organoid model, which further increased the translational significance of anti-CD47 antibody in NASH treatment.

Material and methods

Animals

All the experiments involving mice conformed to the National Institutes of Health Guide for the Care and Use of Laboratory Animals and were approved by the University of Kentucky Institutional Animal Care and Use Committee. All animals were housed in a pathogen-free environment with a light-dark cycle. Male eight-week-old C57BL/6 wild type (WT) mice (The Jackson Laboratory; Bar Harbor, ME) were fed with AMLN diet (40% kcal from fat, 20% kcal from fructose, and 2% kcal from cholesterol D09100301; Research Diets, Inc, NJ) for 20 weeks to induce NASH. The NASH group mice were then divided into two groups and injected every other day with control IgG (from BioXcell, Catalog #BE0083) or monoclonal CD47 antibody (from BioXcell, Catalog # BE0283, Clone MIAP410 (isotype: mouse IgG1, k) for *in vivo* use, 200 μg/mouse) by i.p. After treatment, mice were euthanized and collected blood and tissues for future analysis. Low fat (LF) diet (10% kcal form fat; D12450B; Research Diets, Inc, NJ) fed mice were also included in the study.

Metabolic analysis

Body weight was measured weekly. At the end of the study, body composition was measured by NMR spectroscopy (Echo MRI) [9]. Two weeks prior to the end of study, mice were placed in TSE LabMaster chambers (TSE systems) individually for 5 days for measurement of food intake, water intake and indirect calorimetry.

Liver histological Analysis and immunohistochemical staining

Liver tissues were fixed in 4% neutral buffered formalin and embedded in paraffin. The 5 μm of paraffin sections were stained with Hematoxylin and eosin (H&E), Masson's trichrome, and Sirius red by using the service provided by COBRE Pathology Core at University of Kentucky. The slides were evaluated for fatty changes, inflammation and fibrosis and scored as previously described [10,11]. In addition, the paraffin sections from above were deparaffinized, rehydrated in graded mixtures of ethanol/water, pretreated by boiling in citrate buffer (pH 6.0) and endogenous peroxidase activity was blocked with 3% H_2O_2 for 30 min at room temperature (RT). The paraffin sections were blocked with 5% of BSA blocking solution for 1 hr and incubated with CD11b-Alexa 647 antibody (AbD Serotec, Raleigh, NC) overnight. Next day, the sections were washed and mounted with mounting solution including DAPI. Images were acquired with fluorescent microscope (Eclipse 80i, Nikon) and CD11b positive cells were counted in 9-12 of image fields per group. In addition, some liver paraffin sections were stained with anti-F4/80 antibody (Thermo Fisher Scientific; Waltham, MA), anti-Collagen I antibody (Abcam; Cambridge CB20AX, UK), or anti-neutrophil antibody (Abcam; Cambridge CB20AX, UK), followed by incubation with biotinylated secondary antibody, peroxidase substrate diaminobenzidine (Vector Lab) and counterstaining with hematoxylin. Images were acquired with a Nikon Edipse 55i microscope. Neutrophils were counted in 9-12 of image fields per group. F4/80 positive cells were counted and normalized with counted nuclei. Collagen I positive staining areas were determined as previously described [12].

Lipid Analysis

Plasma total cholesterol and triglyceride, and hepatic cholesterol and triglyceride concentrations were determined enzymatically with Wako kits (Richmond, USA). For analysis of hepatic lipid, approximately 50 mg of liver was placed into 500 μl of chilled Krebs Ringer Phosphate buffer (118 mM NaCl, 5 mM KCl, 13.8 mM $CaCl_2$, 1.2 mM $MgSO_4$, 0.016% KH_2PO_4, 0.211% $NaHCO_2$) and each sample was sonicated for ten times (30 seconds/time).

Blood parameter analysis

At the end of study, blood samples were obtained via retro-orbital bleeding and hematology analysis was performed by using Hemavet 950FS. In addition, liver function was analyzed by determination of plasma alanine aminotransferase (ALT) and aspartate aminotransferase (AST) levels by using ALT and AST assay kit (Connecticut, USA). Blood glucose levels were measured by using glucometer. Plasma insulin levels were measured by using ELISA Kit (Crystal Chem USA, IL).

3D human NASH organoid model with or without anti-CD47 antibody treatment

A 3D human NASH *in vitro* model was established as previously described [13,14]. Human hepatocytes (from Lonza), THP1 derived macrophages (from ATCC) and human stellate cells (HSC, from Zenbio, NA) (total 3,000 seeding cells/well, at ratio 4:1:1, this ratio was chosen to give the best resemblance of the native cellular distribution in liver) were co-cultured using the Corning U-bottom ultra-low attachment plate and the scaffold-free 3D spheroid microtissues were generated after 5-7 days of culture. The 3D spheroid was then treated with DMEM media containing 1% BSA, palmitate (0.5 mM), high glucose (30 mM) and LPS (2 μg/ml) (called NASH inducing media) to mimic NASH environment for additional 5-10 days to allow inducing proinflammatory and profibrogenic phenotype [13,14]. To determine whether anti-CD47 antibody treatment can attenuate hepatic organoid NASH progression, 3D spheroid was treated with NASH inducing media for 5 days and then treated for additional 5 days in the presence of control IgG or anti-CD47 antibody (20 μg/ml). After treatment, cells were harvested and qPCR was performed to determine the expression of genes related to inflammation and fibrosis. In addition, organoids were harvested for Oil Red O staining and triglyceride measurement. Briefly, for oil red O staining, organoids were fixed with 4% PFA and stained with 0.5% Oil red O in 60% isoprophyl alcohol. For triglyceride levels, the organoids were lysed in 100 μl of chilled Krebs Ringer Phosphate buffer and were measured enzymatically by colorimetric methods with Wako kit. For immunofluorescence staining, organoid was fixed with 4% PFA for 10 min and blocked in 5% BSA blocking solution for 1 hr. After that, organoid was incubated with anti-collagen I (Novus Biologicals, 1:100), anti-α-SMA (Sigma, 1:100), anti-GFAP (Abcam, 1:100), or anti-CD68 (Novus Biologicals, 1:100) overnight at 4 °C. After washing, slides were incubated with 1:200 secondary antibody (rabbit-Alexa 488 for collagen I, mouse-Alexa 568 for α-SMA, mouse-Alexa 568 for GFAP, and mouse-Alexa 488 for CD68), and mounted with mounting medium including DAPI. The images were taken with Nikon A1R confocal microscope at X10 (scale bar = 200 μm).

Western Blotting

Western blotting was performed as previously described [15,16]. Briefly, proteins were isolated from cells or tissues and were resolved on SDS-PAGE. Proteins were then transferred to nitrocellulose (NC) membrane. The membrane was blocked in phosphate buffered saline solution with 0.05% Tween 20 (PBST, pH 7.4) containing 5% BSA (Sigma-Aldrich; St. Louis, MO) for 1-3 hr, and then incubated with primary antibodies against NF-kB (Santa Cruz, dilution 1:1000) or smooth muscle α-Actin (Sigma, dilution 1:2000) in PBST containing 5% BSA at 4°C overnight. After the incubation, the membrane was washed four times with PBST and incubated with secondary antibody in PBST with 5 % non-fat dry milk (Bio-Rad Laboratories, Hercules, CA) for 1 hr at room temperature. After subsequent three-time washing in PBST, the membrane was washed once in PBS and developed using Pierce ECL Western Blotting Substrate (Thermo Fisher Scientific; Waltham, MA) and exposed to CL-X films (Thermo Fisher Scientific; Waltham, MA).

RNA Isolation and qPCR Analysis

Total RNA was isolated from mouse liver tissues or cells using TRIzol Reagent (Invitrogen Life Technology; Carlsbad, CA). RNA was reverse transcribed to cDNA by High Capacity cDNA Reverse Transcription Kit (Invitrogen, Carlsbad, CA). Real-time quantitative PCR was performed on a MyiQ Real-time PCR Thermal Cycler (Bio-Rad) with SYBR Green PCR Master Kit (Qiagen, Valencia, CA). Relative mRNA expression was calculated using the MyiQ system software as previous reported [17] and normalized to GAPDH or β-actin levels. All primer sequences utilized in this study are found in Table 2.

Statistical analysis

Statistical analysis was performed using Prism version 8.0.2 (GraphPad Software, San Diego, CA). All data are presented as the mean ± SEM. Individual pairwise comparisons were analyzed by two-sample, two-tailed Student's t-test unless otherwise noted, with $P<0.05$ was regarded as significant. One-way analysis of variance was used when multiple comparisons were made, followed by Dunnett's t test for multiple comparisons to a control. N numbers are listed in figure legends.

Results

Anti-CD47 antibody administration did not affect body weight, plasmid lipid levels, or blood glucose levels in mice with established NASH

Several dietary and genetic rodent NAFLD/NASH models have been used in the field. Given the complex etiology and pathology of human NAFLD, to date, a perfect model that recapitulates all pathological features of human NASH has not been developed. However, dietary animal models rank the highest relevance to human NAFLD and widely used by researches. The AMLN diet (40% fat from trans-fat, 22% fructose, and 2% cholesterol) has been used to induce advanced stages of NAFLD including NASH and hepatic fibrosis after 20-30 weeks' feeding, which faithfully recapitulates key features of human NASH [18-20]. Using this well-established AMLN diet induced preclinic mouse NASH model, we determined the potential therapeutic effect of anti-CD47 antibody on NASH progression.

Consistent with previous reports [18-20], our results showed that AMLN diet fed mice developed obesity, type 2 diabetes and NASH. Four weeks of anti-CD47 treatment had no effect on mice body weight or fat mass changes (Fig. 1A-C). Plasma total cholesterol and free cholesterol levels, blood glucose or insulin levels were comparable between NASH-CD47 antibody group and NASH-control IgG group (Fig. 1D-E). In addition, anti-CD47 antibody treatment did not affect mice food intake or energy expenditure as determined by TSE System (Figure_1_SuppInfo).

Anti-CD47 antibody administration significantly attenuated hepatic inflammation and fibrosis without alteration of liver lipid levels in mice with established NASH

We determined whether anti-CD47 antibody treatment attenuates NAFLD/NASH progression by analyzation of liver histology, steatosis, inflammation and fibrosis markers. As shown in Fig. 2A-C, control NASH mice had increased liver size, hepatic lipid levels including triglyceride, total and free cholesterol levels, and upregulated genes relating to liver lipid metabolisms such as FASN, SCD-1 ACC, Shrebp1c, HMGCR, or HMGCs as compared to LF group. However, anti-CD47 antibody treated NASH mice had similar liver weight and lipid levels as compared to NASH control mice, suggesting that anti-CD47 antibody treatment had no effect on hepatic steatosis development, which was further confirmed by liver H&E staining (Fig. 2D). In addition, plasma ALT level had a trend of reduction in anti-CD47 treatment group as compared to NASH-IgG group (Figure_2_SuppInfor). Although anti-CD47 antibody treatment did not affect steatosis, histology scores of liver inflammation and fibrosis was significantly reduced in NASH-CD47 antibody group as compared to NASH-control group (Fig. 2D). Moreover, qPCR data showed that anti-CD47 antibody treatment downregulated AMLN diet induced expression of liver proinflammatory cytokines (e.g. IL-1β, MCP-1, TNF-α) or macrophage markers (e.g. F4/80, CD11b) (Fig. 3A). CD 47 antibody treatment mediated down-regulation of F4/80 or CD11b expression in NASH livers was further supported by immunofluorescent staining data (Fig. 3B, C), suggesting that infiltrated or resident liver macrophages were reduced by CD47 antibody treatment. In addition, hepatic infiltrated neutrophils (Fig. 3E) and liver NF-kB levels were also reduced by CD47 antibody treatment (Fig. 3D).

In addition to liver inflammation, liver fibrosis was analyzed by trichome and sirius red staining of liver sections. As shown in Fig. 4A, both trichrome and Sirius red positive staining areas were increased in NASH control group as compared to LF group, which was attenuated by anti-CD47 antibody treatment. This is consistent with the reduced expression of fibrosis makers such as α-SMA (smooth muscle actin) and Collagen I in CD47 antibody treatment group (Fig. 4C, D). We also found transcript levels of Timp1, a positive regulator of fibrogenesis [21], to be substantially augmented in NASH control group and attenuated by anti-CD47 treatment (Fig. 4B). In vitro studies further confirmed the inhibitory effect of anti-CD47 antibody treatment on hepatic stellate cell activation (Fig. 4_SuppInfo). Taken together, these data suggest that anti-CD47 antibody administration prevents NASH progression by reducing infiltrated or resident liver macrophages and liver proinflammatory cytokines production as well as attenuating stellate cell activation and excess collagen deposition in liver.

Effect of anti-CD47 antibody treatment on mice blood profile

Since CD47 is ubiquitously expressed in many different cell types, during anti-CD47 antibody treatment, antibody may encounter a vast pool of CD47 on red blood cells and other vascular cells and may result in anemia. Therefore, at the end of the study, a complete blood profile was performed by using Hemavet 950FS. As shown in Table 1, red blood cell number was indeed reduced in NASH-anti CD47 group as compared to control groups. Interestingly, we also found that white blood cell (WBC) count especially neutrophil and lymphocytes count was significantly increased in NASH-control IgG group as compared to LF group. This was abolished by anti-CD47 antibody treatment. Increased circulating neutrophil frequency has been shown in NASH patients and positively correlates with NASH activity scores [22,23]. Therefore, our data suggests that anti-CD47 treatment negatively regulates circulating neutrophils number and liver infiltrated neutrophils, contributing to the observed reduced liver inflammation (Fig. 3).

Anti-CD47 antibody treatment inhibited the development of inflammation and fibrosis in 3D human NASH organoid

To determine the human relevance of anti-CD47 antibody treatment in NASH, a 3D human NASH *in vitro* model was used [13,14]. Human hepatocytes, macrophages, and stellate cells were co-cultured using the Corning U-bottom ultra-low attachment plate to form scaffold-free 3D spheroid microtissues after 5-7 days of culture as demonstrated under phase contrast microscope (Fig. 5A). The 3D spheroid were then treated with NASH inducing media (DMEM media containing 1% BSA, palmitate (0.5 mM), high glucose (30 mM) and LPS (2 μg/ml) to mimic NASH environment) for 5-10 days to induce proinflammatory and profibrogenic phenotype (Fig. 5B). To determine whether anti-CD47 antibody treatment can attenuate hepatic organoid NASH progression, 3D spheroid was treated with NASH inducing media for 5 days and then treated for additional 5 days in the presence of control IgG or anti-CD47 antibody (20 μg/ml). After treatment, cells were harvested for qPCR. As shown in Fig. 5C, NASH media stimulated the expression of IL-1β, α-SMA, and Collagen I, which was attenuated by anti-CD47 antibody treatment. Fluorescence images showed that a-SMA or Collagen I positive staining was reduced by anti-CD47 antibody treatment (Fig. 5D). In addition, anti-CD47 treatment did not affect triglyceride levels. The number of macrophages or stellate cells was comparable between IgG and anti-CD47 treated organoids as demonstrated by immunofluorescence staining and qPCR (Fig. 5_SuppInfo). Together these data demonstrated that anti-CD47 antibody treatment attenuated NASH media stimulated inflammation and fibrosis in human liver organoids, supporting the human relevance of anti-CD47 antibody treatment in NASH.

Discussion

In this study, the therapeutic potential of anti-CD47 antibody in NASH progression was tested by using both AMLN diet-induced NASH mouse model and 3D human NASH organoid model. These two models make our study more human relevant and translational. We demonstrated that four weeks of anti-CD47 antibody treatment attenuated liver inflammation and fibrosis in mice with established NASH. This protective effect was

also seen in human 3D NASH organoid, suggesting that CD47 blocking antibody might be a new therapeutic option for NASH.

CD47 has been implicated in immunity, self-recognition and stress response [3-7]. Recently emerging evidence suggest that CD47 and its ligand-TSP1 play a novel role in the development of obesity and its associated metabolic diseases including NAFLD/NASH [8,9,24-26]. Studies from our lab have demonstrated that genetic deletion of CD47 had increased brown adipose tissue function (e.g. increased heat production) and energy utilization, which protected mice from four months of high fat diet feeding induced obesity and liver steatosis [9]. However, in this study, we found that anti-CD47 antibody treatment did not increase mice energy expenditure or decrease body weight gain during AMLN diet feeding period. Plasma glucose or lipid level was not affected, either. This indicates that four weeks of anti-CD47 antibody treatment might be not long enough to combat established obesity and diabetes that are associated with NAFLD/NASH [27-30]. AMLN diet induced increase in liver lipid levels or steatosis were not improved by short-term anti-CD47 antibody treatment, either. Interestingly, a recent study showed that global CD47 gene deletion exacerbated liver lipid metabolism during eight months of high fat diet feeding period by downregulation of PPARα pathway [25]. This chronic feeding study suggests that basal level of CD47 expressed on hepatocytes might be indispensable for maintaining normal hepatocyte lipid metabolism function. In our study, antibody treatment may only partially block CD47 signaling on hepatocytes and thus steatosis did not get worse in antibody treated mice. Further studies are warranted to definitively determine the role of CD47 in regulating hepatocyte lipid metabolism.

Although the steatosis was not altered by CD47 antibody treatment in our study, liver inflammation including proinflammatory cytokine production and the associated activation of NF-κB was significantly reduced in antibody treated NASH group of mice. This is partially due to decreased number of infiltrated immune cells (e.g. macrophages, neutrophils et al) and /or their activation status in livers. Cumulative evidence has suggested that macrophages play an important role in NAFLD/NASH pathogenesis [31]. Moreover, hepatic macrophages, a heterogeneous and dynamic population including kupffer cells and infiltrating monocyte-derived macrophages, undergo expansion and functional changes during NASH development [32-38]. Therefore, targeting macrophage infiltration and/or activation might be a treatment option for NASH. Consistently, our results showed that CD47 antibody blockade reduced hepatic monocyte/macrophages infiltration. This is partially due to reduced liver MCP1 levels. MCP1 is a potent chemo-attractive mediator for monocyte/macrophages and could be produced by many liver cell types such as hepatocytes, Kupffer cells, stellate cells et al. Under NAFLD/NASH conditions, anti-CD47 antibody treatment may block CD47 signaling on these impaired liver cells and inhibit MCP1 expression and secretion from these cells, leading to reduced hepatic monocyte/macrophage recruitment. In addition, CD47 is a receptor for thrombospondin1 (TSP1). TSP1 signaling through CD47 has been shown to control macrophage recruitment and activation in a liver ischemia/reperfusion injury model [39,40]. Upregulated liver TSP1 signaling has also been demonstrated in NAFLD/NASH mouse model and human NASH patients in our previous studies[24]. Therefore, anti-CD47 antibody treatment may block TSP1's effect on

macrophage migration and activation in NAFLD/NASH livers, contributing to the reduced liver inflammation.

In addition to the effect on macrophages, interestingly, CD47 blockade reduced circulating neutrophils in NASH mice. Possible causes for this finding include: 1) anti-CD47 treatment might block the interaction between neutrophil CD47 and SIRPα on macrophages and then stimulate the phagocytosis of neutrophils by macrophages [41] and 2) anti-CD47 treatment could similarly stimulate the phagocytosis of bone marrow cells by macrophages, leading to the impairment in neutrophil output [42]. However, the exact underlying mechanisms would need to be further investigated. The reduced infiltrated neutrophils into livers were also seen in the anti-CD47 antibody treatment group, which is consistent with the role of CD47 in regulating neutrophil chemotaxis [41,43,44]. The involvement of neutrophil in NASH development/progression has been supported by many studies. For instance, the circulating neutrophil to lymphocyte ratio has been found to be high in NASH patients with advanced fibrosis [45]. Increased circulating neutrophils in NASH patients can modulate $CD^{4+}$and CD^{8+} T cell function, contributing to NASH progression [22]. Neutrophil-derived myeloperoxidase (MPO) has been shown to be associated with hepatic cholesterol accumulation, inflammation, and fibrosis [46]. Moreover, systemic neutrophil depleted mice have shown less hepatic toxicity and inflammation in early stage of NASH [47], but impair spontaneous resolution of liver inflammation and fibrosis [48]. Collectively, these studies highlight the contribution of increased circulating and/or hepatic infiltrated immune cells (e.g. macrophages, neutrophils et al) to NASH development/progression. By reducing neutrophils or macrophages infiltrating into livers during NASH development, CD47 antibody treatment reduces liver inflammation.

In this study, anti-CD47 treatment also inhibited hepatic stellate cell activation and excess extracellular matrix production, leading to the partial resolution of liver fibrosis under NASH conditions. The inhibitory effect of CD47 blockade on hepatic stellate cell activation was further confirmed in our *in vitro* studies. We found that CD47 antibody pretreatment attenuated TGF-β1- induced α-SMA production in hepatic stellate cell. TGF-β1 is a key driver for liver fibrogenesis. Although CD47-antibody treatment did not affect total TGF-β1 expression in NASH livers (Fig. 4B), the downstream TGF-β signaling (e.g. p-SMAD2) and the resultant fibrogenic program in stellate cells might be inhibited by anti-CD47 antibody treatment [49]. This warrants further investigation in the future.

In summary, our study indicates that four weeks of anti-CD47 antibody administration could prevent NASH progression by partial resolution of liver inflammation and fibrosis in both diet-induced NASH mouse model and human NASH organoid. This study suggests that anti-CD47 blocking antibody could be a new therapeutic option for NASH.

Supplementary Material

Refer to Web version on PubMed Central for supplementary material.

Funding Statement:

This work was supported by the Department of Veterans Affairs Merit Review Award (I01BX004252, to SW), the National Institutes of Health (NIH) Grant (DK098176, to SW), and an Institutional Development Award (IDeA) from the National Institute of General Medical Sciences of the National Institutes of Health under grant number P30 GM127211.

Data Availability Statement:

The data that support the findings of this study are available from the corresponding author upon reasonable request.

List of abbreviations:

NAFLD	non-alcoholic fatty liver diseases
NASH	non-alcoholic steatohepatitis
ALT	plasma alanine aminotransferase
AST	aspartate aminotransferase
TG	total triglyceride
TC	total cholesterol
FC	free cholesterol
α-SMA	α-smooth muscle actin

References

1. Loomba R, Sanyal AJ. The global NAFLD epidemic. Nature reviews Gastroenterology & hepatology. 2013;10(11):686–690. [PubMed: 24042449]
2. Romero-Gomez M, Zelber-Sagi S, Trenell M. Treatment of NAFLD with diet, physical activity and exercise. J Hepatol. 2017.
3. Barclay AN, Van den Berg TK. The interaction between signal regulatory protein alpha (SIRPalpha) and CD47: structure, function, and therapeutic target. Annual review of immunology. 2014;32:25–50.
4. Rogers NM, Yao M, Novelli EM, Thomson AW, Roberts DD, Isenberg JS. Activated CD47 regulates multiple vascular and stress responses: implications for acute kidney injury and its management. Am J Physiol Renal Physiol. 2012;303(8):F1117–1125. [PubMed: 22874763]
5. Isenberg JS, Qin Y, Maxhimer JB, et al. Thrombospondin-1 and CD47 regulate blood pressure and cardiac responses to vasoactive stress. Matrix Biol. 2009;28(2):110–119. [PubMed: 19284971]
6. Isenberg JS, Shiva S, Gladwin M. Thrombospondin-1-CD47 blockade and exogenous nitrite enhance ischemic tissue survival, blood flow and angiogenesis via coupled NO-cGMP pathway activation. Nitric Oxide. 2009;21(1):52–62. [PubMed: 19481167]
7. Isenberg JS, Frazier WA, Krishna MC, Wink DA, Roberts DD. Enhancing cardiovascular dynamics by inhibition of thrombospondin-1/CD47 signaling. Current drug targets. 2008;9(10):833–841. [PubMed: 18855617]
8. Memetimin H, Li D, Tan K, et al. Myeloid-specific deletion of thrombospondin 1 protects against inflammation and insulin resistance in long-term diet-induced obese male mice. Am J Physiol Endocrinol Metab. 2018;315(6):E1194–E1203. [PubMed: 30351986]

9. Maimaitiyiming H, Norman H, Zhou Q, Wang S. CD47 deficiency protects mice from diet-induced obesity and improves whole body glucose tolerance and insulin sensitivity. Sci Rep. 2015;5:8846. [PubMed: 25747123]
10. Kim M, Yang SG, Kim JM, Lee JW, Kim YS, Lee JI. Silymarin suppresses hepatic stellate cell activation in a dietary rat model of non-alcoholic steatohepatitis: analysis of isolated hepatic stellate cells. Int J Mol Med. 2012;30(3):473–479. [PubMed: 22710359]
11. Liang W, Menke AL, Driessen A, et al. Establishment of a general NAFLD scoring system for rodent models and comparison to human liver pathology. PLoS One. 2014;9(12):e115922. [PubMed: 25535951]
12. Crowe AR, Yue W. Semi-quantitative Determination of Protein Expression using Immunohistochemistry Staining and Analysis: An Integrated Protocol. Bio Protoc. 2019;9(24).
13. Mukherjee S, Zhelnin L, Sanfiz A, et al. Development and validation of an in vitro 3D model of NASH with severe fibrotic phenotype. American journal of translational research. 2019;11(3):1531–1540. [PubMed: 30972180]
14. Prestigiacomo V, Weston A, Messner S, Lampart F, Suter-Dick L. Pro-fibrotic compounds induce stellate cell activation, ECM-remodelling and Nrf2 activation in a human 3D-multicellular model of liver fibrosis. PLoS One. 2017;12(6):e0179995. [PubMed: 28665955]
15. Helsley RN, Sui Y, Park SH, et al. Targeting IkappaB kinase beta in Adipocyte Lineage Cells for Treatment of Obesity and Metabolic Dysfunctions. Stem Cells. 2016;34(7):1883–1895. [PubMed: 26991836]
16. Sui Y, Liu Z, Park SH, et al. IKKbeta is a beta-catenin kinase that regulates mesenchymal stem cell differentiation. JCI Insight. 2018;3(2):e96660.
17. Li Y, Tong X, Rumala C, Clemons K, Wang S. Thrombospondin1 deficiency reduces obesity-associated inflammation and improves insulin sensitivity in a diet-induced obese mouse model. PLoS One. 2011;6(10):e26656. [PubMed: 22039525]
18. Clapper JR, Hendricks MD, Gu G, et al. Diet-induced mouse model of fatty liver disease and nonalcoholic steatohepatitis reflecting clinical disease progression and methods of assessment. American journal of physiology Gastrointestinal and liver physiology. 2013;305(7):G483–495. [PubMed: 23886860]
19. Kristiansen MN, Veidal SS, Rigbolt KT, et al. Obese diet-induced mouse models of nonalcoholic steatohepatitis-tracking disease by liver biopsy. World journal of hepatology. 2016;8(16):673–684. [PubMed: 27326314]
20. Trevaskis JL, Griffin PS, Wittmer C, et al. Glucagon-like peptide-1 receptor agonism improves metabolic, biochemical, and histopathological indices of nonalcoholic steatohepatitis in mice. American journal of physiology Gastrointestinal and liver physiology. 2012;302(8):G762–772. [PubMed: 22268099]
21. Thiele ND, Wirth JW, Steins D, et al. TIMP-1 is upregulated, but not essential in hepatic fibrogenesis and carcinogenesis in mice. Sci Rep. 2017;7(1):714. [PubMed: 28386095]
22. Antonucci L, Porcu C, Timperi E, Santini SJ, Iannucci G, Balsano C. Circulating Neutrophils of Nonalcoholic Steatohepatitis Patients Show an Activated Phenotype and Suppress T Lymphocytes Activity. J Immunol Res. 2020;2020:4570219. [PubMed: 32671116]
23. Liu K, Wang FS, Xu R. Neutrophils in liver diseases: pathogenesis and therapeutic targets. Cell Mol Immunol. 2021;18(1):38–44. [PubMed: 33159158]
24. Gwag T, Reddy Mooli RG, Li D, Lee S, Lee EY, Wang S. Macrophage-derived thrombospondin 1 promotes obesity-associated non-alcoholic fatty liver disease. JHEP Rep. 2021;3(1):100193. [PubMed: 33294831]
25. Tao HC, Chen KX, Wang X, et al. CD47 Deficiency in Mice Exacerbates Chronic Fatty Diet-Induced Steatohepatitis Through Its Role in Regulating Hepatic Inflammation and Lipid Metabolism. Frontiers in immunology. 2020;11:148. [PubMed: 32158445]
26. Varma V, Yao-Borengasser A, Bodles AM, et al. Thrombospondin-1 is an adipokine associated with obesity, adipose inflammation, and insulin resistance. Diabetes. 2008;57(2):432–439. [PubMed: 18057090]

27. Garcia-Monzon C, Martin-Perez E, Iacono OL, et al. Characterization of pathogenic and prognostic factors of nonalcoholic steatohepatitis associated with obesity. J Hepatol. 2000;33(5):716–724. [PubMed: 11097478]
28. Ayonrinde OT, Oddy WH, Adams LA, et al. Infant nutrition and maternal obesity influence the risk of non-alcoholic fatty liver disease in adolescents. J Hepatol. 2017;67(3):568–576. [PubMed: 28619255]
29. Tilg H, Moschen AR, Roden M. NAFLD and diabetes mellitus. Nat Rev Gastroenterol Hepatol. 2017;14(1):32–42. [PubMed: 27729660]
30. Parry SA, Hodson L. Managing NAFLD in Type 2 Diabetes: The Effect of Lifestyle Interventions, a Narrative Review. Adv Ther. 2020;37(4):1381–1406. [PubMed: 32146704]
31. Kazankov K, Jorgensen SMD, Thomsen KL, et al. The role of macrophages in nonalcoholic fatty liver disease and nonalcoholic steatohepatitis. Nature reviews Gastroenterology & hepatology. 2019;16(3):145–159. [PubMed: 30482910]
32. Krenkel O, Puengel T, Govaere O, et al. Therapeutic inhibition of inflammatory monocyte recruitment reduces steatohepatitis and liver fibrosis. Hepatology (Baltimore, Md). 2018;67(4):1270–1283.
33. McGettigan B, McMahan R, Orlicky D, et al. Dietary Lipids Differentially Shape Nonalcoholic Steatohepatitis Progression and the Transcriptome of Kupffer Cells and Infiltrating Macrophages. Hepatology (Baltimore, Md). 2019;70(1):67–83.
34. Xiong X, Kuang H, Ansari S, et al. Landscape of Intercellular Crosstalk in Healthy and NASH Liver Revealed by Single-Cell Secretome Gene Analysis. Molecular cell. 2019;75(3):644–660 e645. [PubMed: 31398325]
35. Ramachandran P, Dobie R, Wilson-Kanamori JR, et al. Resolving the fibrotic niche of human liver cirrhosis at single-cell level. Nature. 2019;575(7783):512–518. [PubMed: 31597160]
36. Liao CY, Song MJ, Gao Y, Mauer AS, Revzin A, Malhi H. Hepatocyte-Derived Lipotoxic Extracellular Vesicle Sphingosine 1-Phosphate Induces Macrophage Chemotaxis. Frontiers in immunology. 2018;9:2980. [PubMed: 30619336]
37. Krenkel O, Tacke F. Liver macrophages in tissue homeostasis and disease. Nat Rev Immunol. 2017;17(5):306–321. [PubMed: 28317925]
38. Remmerie A, Martens L, Thoné T, et al. Osteopontin Expression Identifies a Subset of Recruited Macrophages Distinct from Kupffer Cells in the Fatty Liver. Immunity. 2020;53(3):641–657 e614. [PubMed: 32888418]
39. Isenberg JS, Maxhimer JB, Powers P, Tsokos M, Frazier WA, Roberts DD. Treatment of liver ischemia-reperfusion injury by limiting thrombospondin-1/CD47 signaling. Surgery. 2008;144(5):752–761. [PubMed: 19081017]
40. Stein EV, Miller TW, Ivins-O'Keefe K, Kaur S, Roberts DD. Secreted Thrombospondin-1 Regulates Macrophage Interleukin-1beta Production and Activation through CD47. Sci Rep. 2016;6:19684. [PubMed: 26813769]
41. Barrera L, Montes-Servín E, Hernandez-Martinez JM, et al. CD47 overexpression is associated with decreased neutrophil apoptosis/phagocytosis and poor prognosis in non-small-cell lung cancer patients. Br J Cancer. 2017;117(3):385–397. [PubMed: 28632731]
42. Jaiswal S, Jamieson CH, Pang WW, et al. CD47 is upregulated on circulating hematopoietic stem cells and leukemia cells to avoid phagocytosis. Cell. 2009;138(2):271–285. [PubMed: 19632178]
43. Liu Y, Buhring HJ, Zen K, et al. Signal regulatory protein (SIRPalpha), a cellular ligand for CD47, regulates neutrophil transmigration. J Biol Chem. 2002;277(12):10028–10036. [PubMed: 11792697]
44. Liu Y, Merlin D, Burst SL, Pochet M, Madara JL, Parkos CA. The role of CD47 in neutrophil transmigration. Increased rate of migration correlates with increased cell surface expression of CD47. J Biol Chem. 2001;276(43):40156–40166. [PubMed: 11479293]
45. Alkhouri N, Morris-Stiff G, Campbell C, et al. Neutrophil to lymphocyte ratio: a new marker for predicting steatohepatitis and fibrosis in patients with nonalcoholic fatty liver disease. Liver Int. 2012;32(2):297–302. [PubMed: 22097893]

46. Rensen SS, Bieghs V, Xanthoulea S, et al. Neutrophil-derived myeloperoxidase aggravates non-alcoholic steatohepatitis in low-density lipoprotein receptor-deficient mice. PLoS One. 2012;7(12):e52411. [PubMed: 23285030]

47. Zang S, Wang L, Ma X, et al. Neutrophils Play a Crucial Role in the Early Stage of Nonalcoholic Steatohepatitis via Neutrophil Elastase in Mice. Cell Biochem Biophys. 2015;73(2):479–487. [PubMed: 27352342]

48. Calvente CJ, Tameda M, Johnson CD, et al. Neutrophils contribute to spontaneous resolution of liver inflammation and fibrosis via microRNA-223. J Clin Invest. 2019;129(10):4091–4109. [PubMed: 31295147]

49. Shimada K, Nakajima A, Ikeda K, Ishibashi K, Shimizu N, Ito K. CD47 regulates the TGF-β signaling pathway in osteoblasts and is distributed in Meckel's cartilage. J Oral Sci. 2011;53(2):169–175. [PubMed: 21712621]

A)

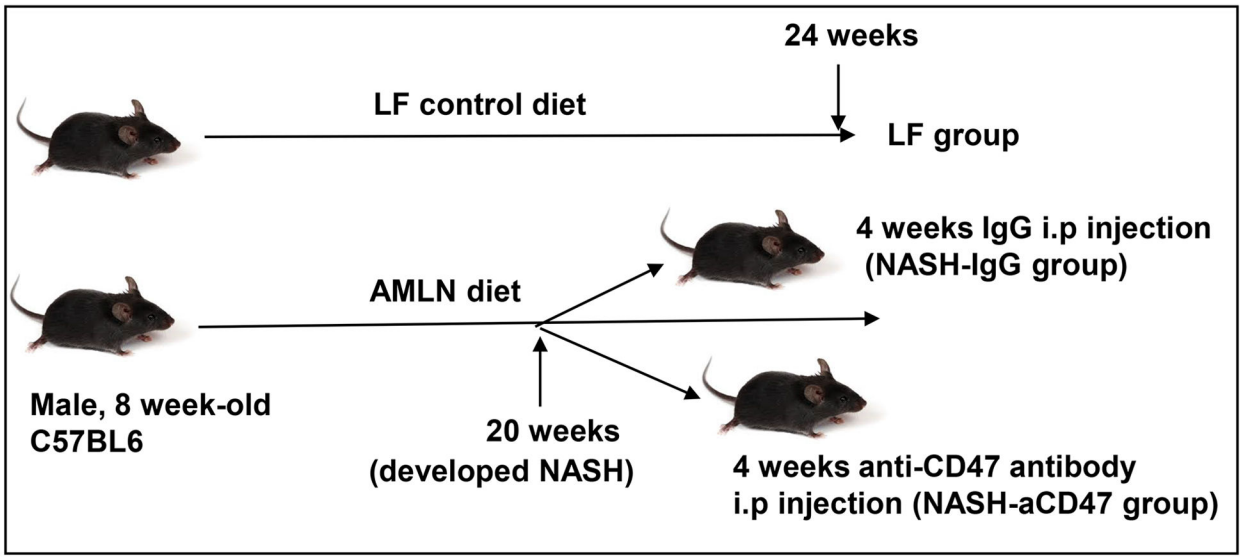

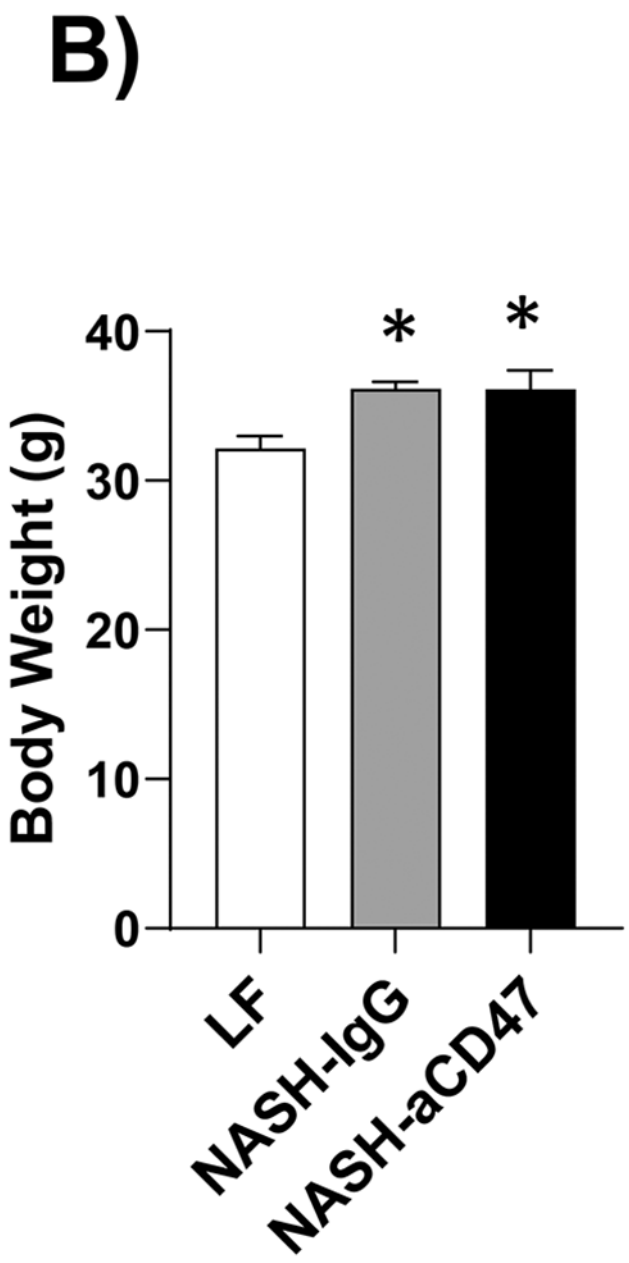

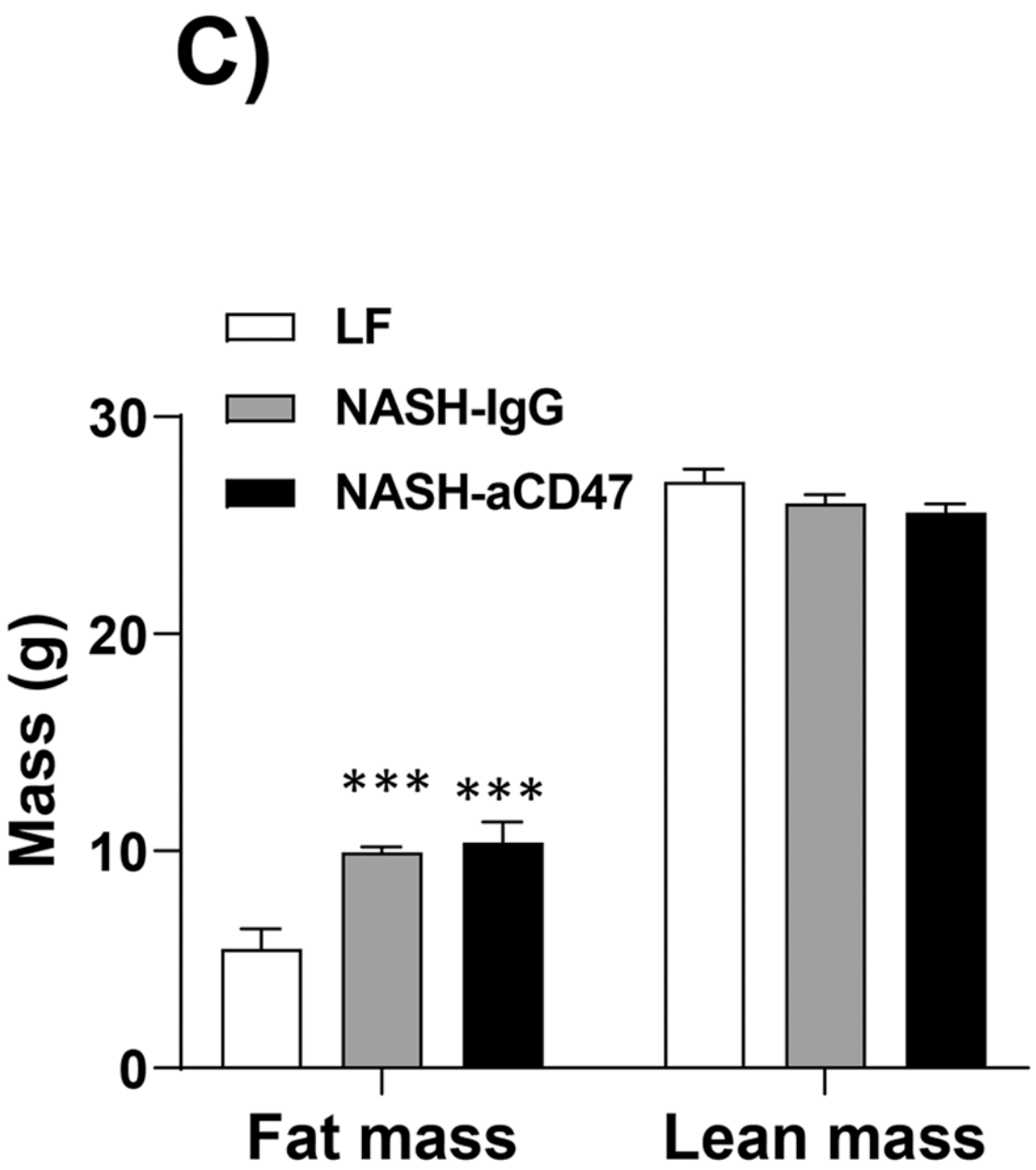

D)

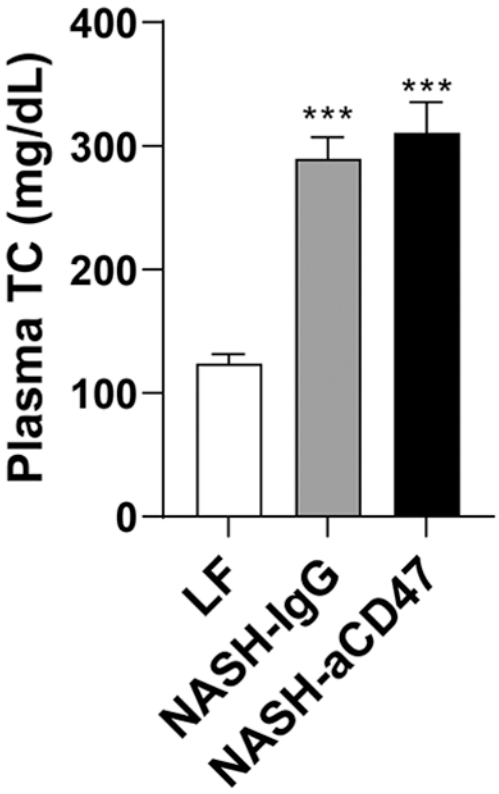

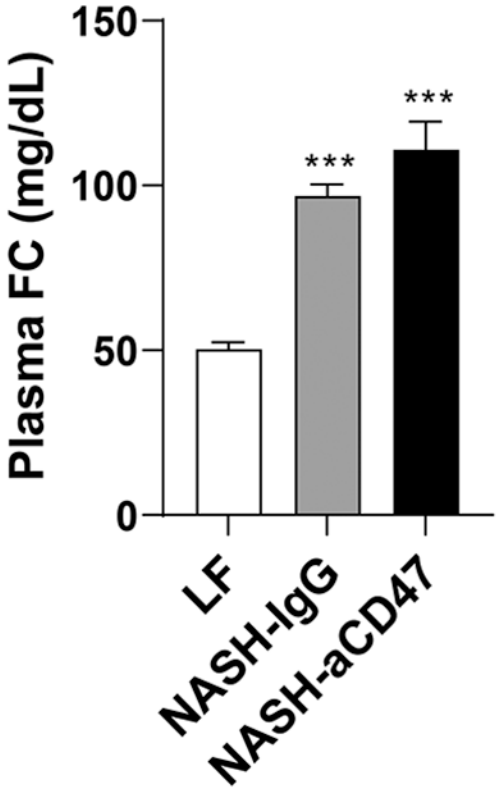

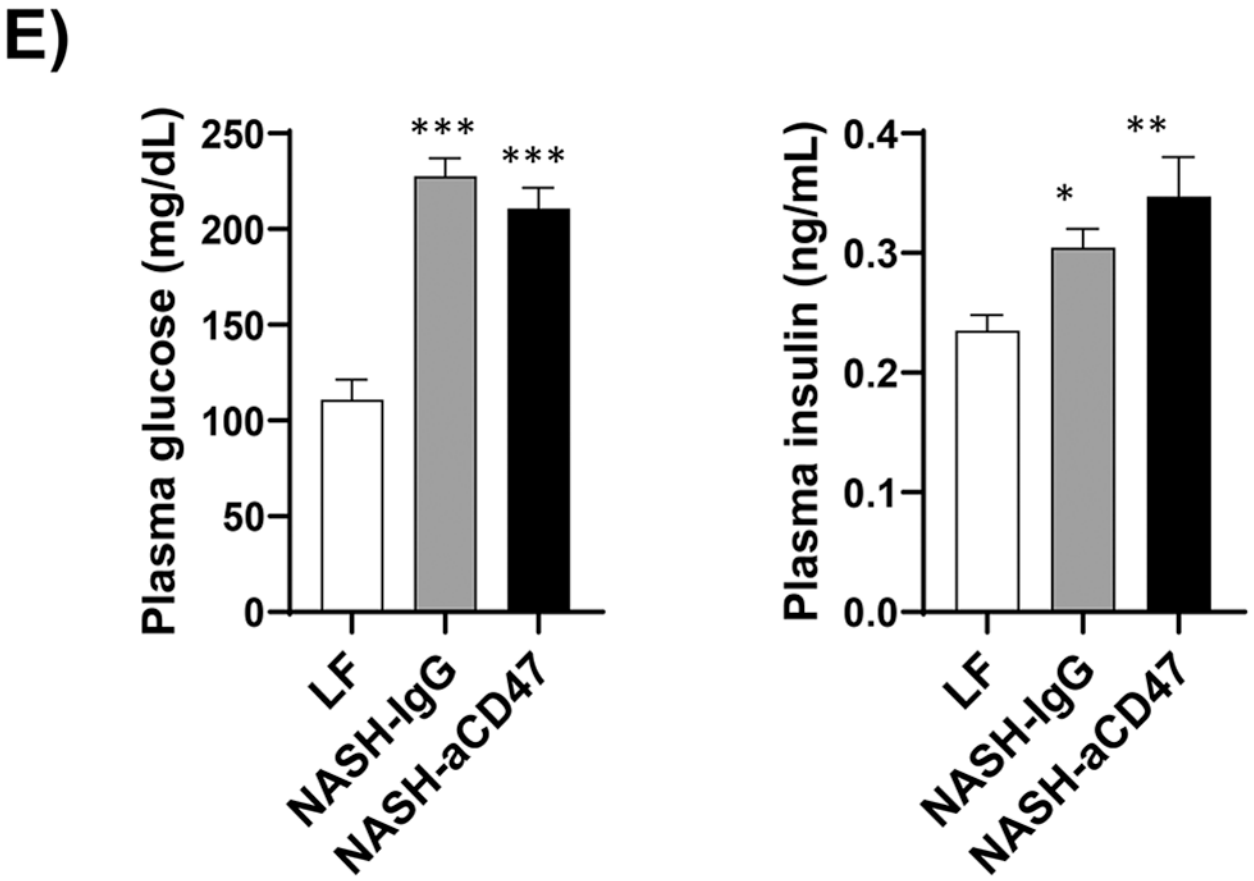

Fig. 1. Anti-CD47 antibody treatment did not affect AMLN diet-induced obesity and other plasma metabolic parameters

C57BL6 male mice (8 weeks-old) were fed with LF or AMLN diet for 20 weeks. AMLN diet-fed mice were then divided into two groups and received intraperitoneal injection of control IgG or anti- CD47 antibody (200 μg/mouse) every other day for 4 weeks. (A) Study Design; (B) Body weight; (C) Body composition; (D) Plasma lipid levels. TC: total cholesterol and FC: free cholesterol; and (E) Plasma overnight fasting glucose and insulin levels. Data are represented as mean ± SEM (n=8 mice/group). **P*<0.05, ** *P*<0.01, and *** *P*<0.001 compared to LF

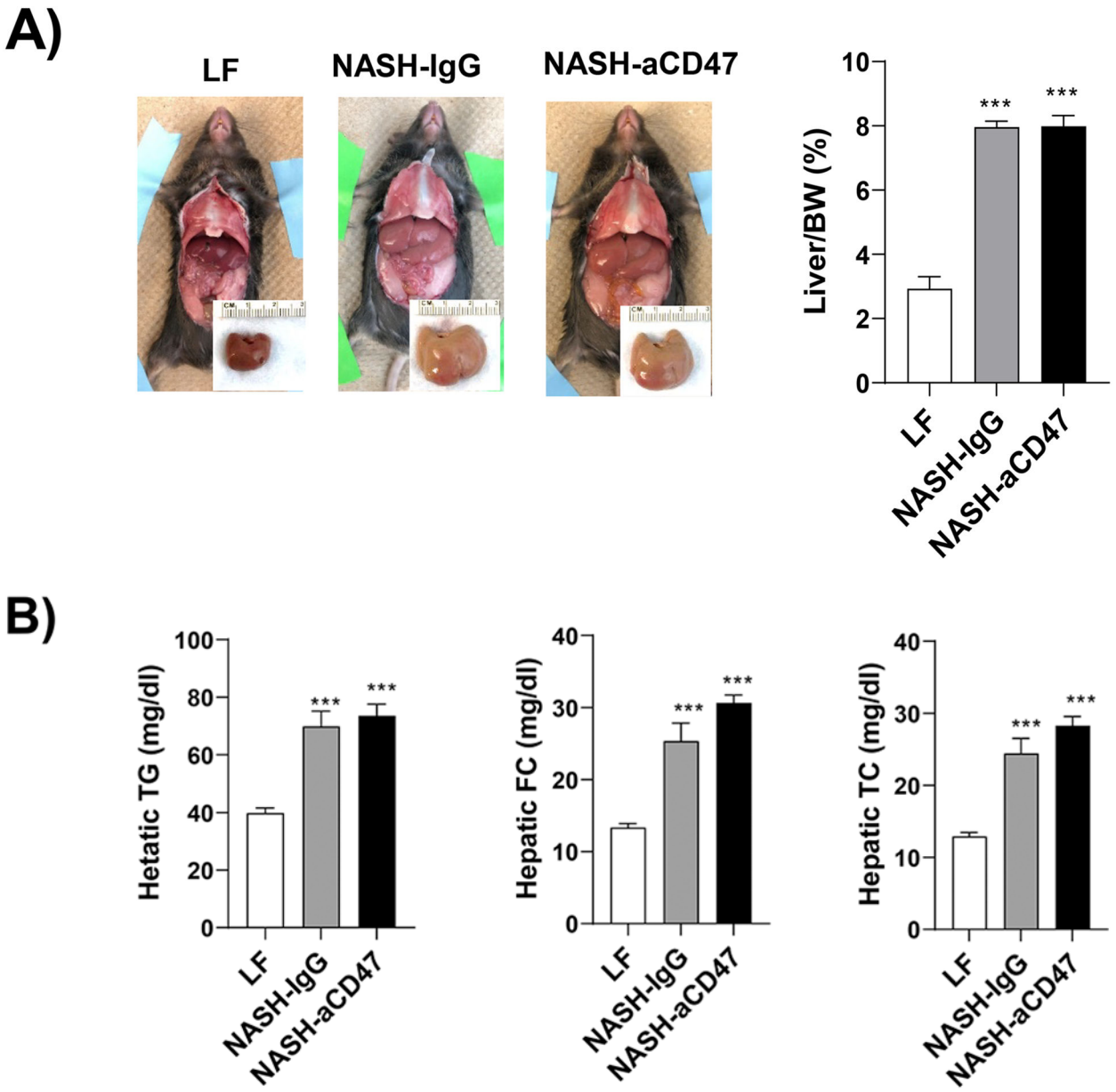

C)

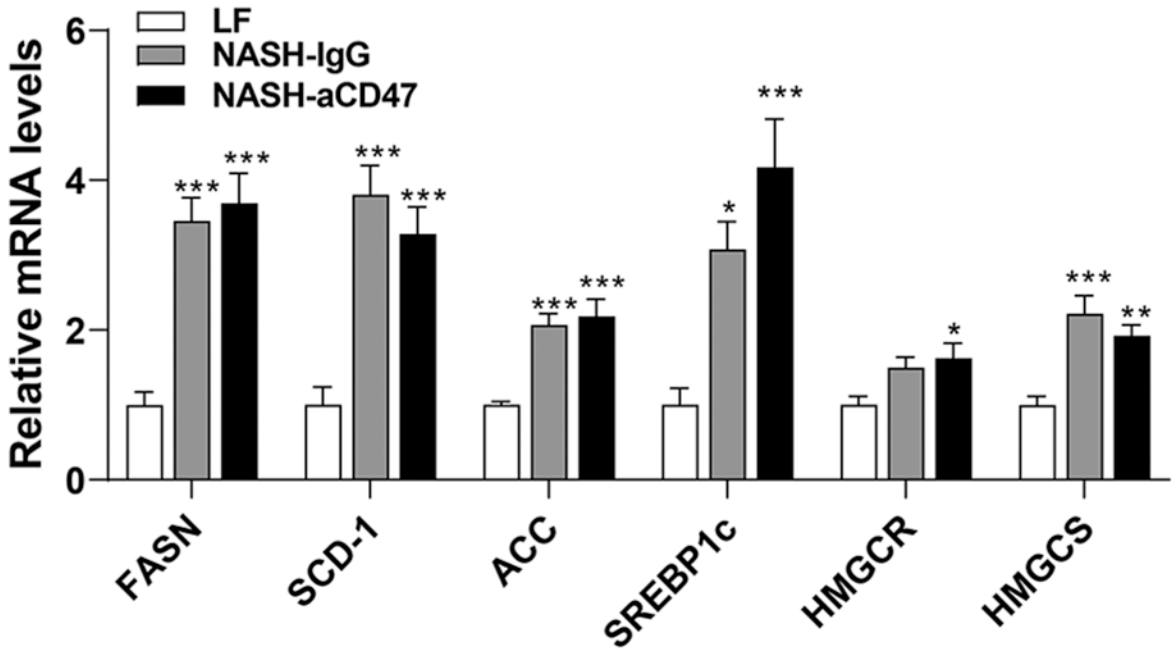

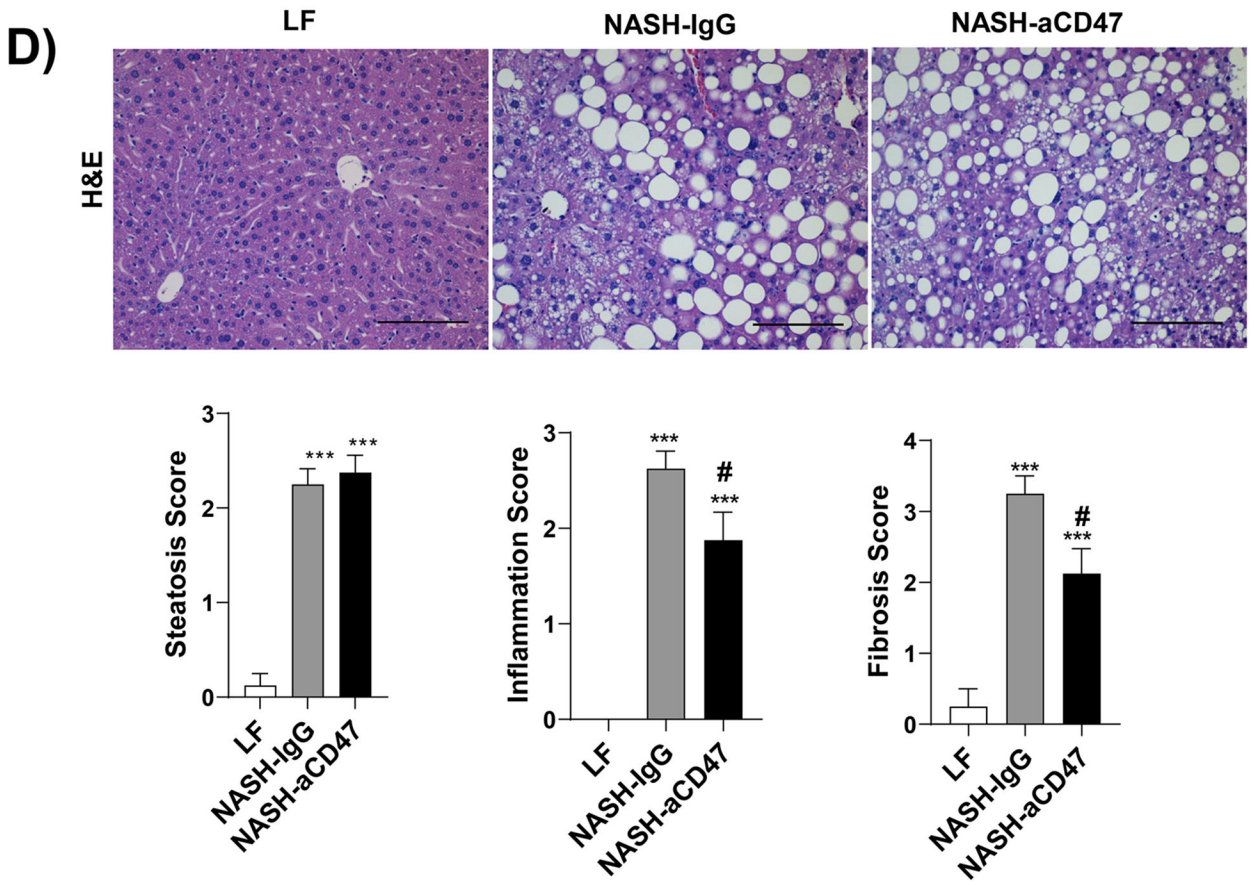

Fig. 2. Anti-CD47 antibody treatment did not improve AMLN diet-induced steatosis

(A)-(B) Representative liver images and liver weight from 3 groups of mice; (C) Hepatic lipid levels and mRNA levels of lipid metabolism related genes in liver by qPCR. TC: total cholesterol; FC: free cholesterol; TG: triglycerides; (D) Representative H&E staining of liver sections (Scale bar=100 μm) and histology scores from 3 groups of mice. Data are represented as mean ± SEM (n=8 mice/group). **P*<0.05, ***P*<0.01, and *** *P*<0.001 compared to LF; #*P*<0.05 compared to NASH-IgG

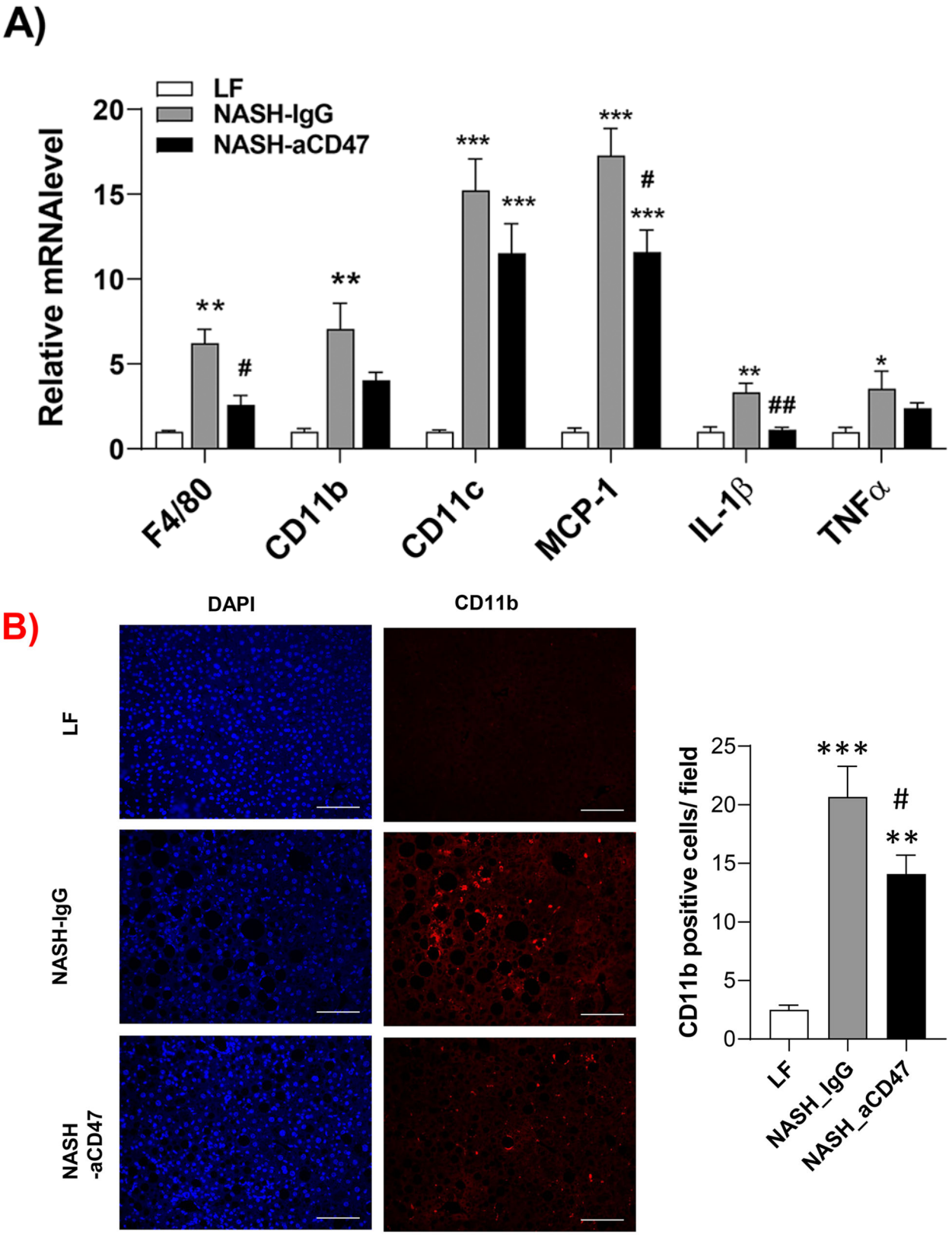

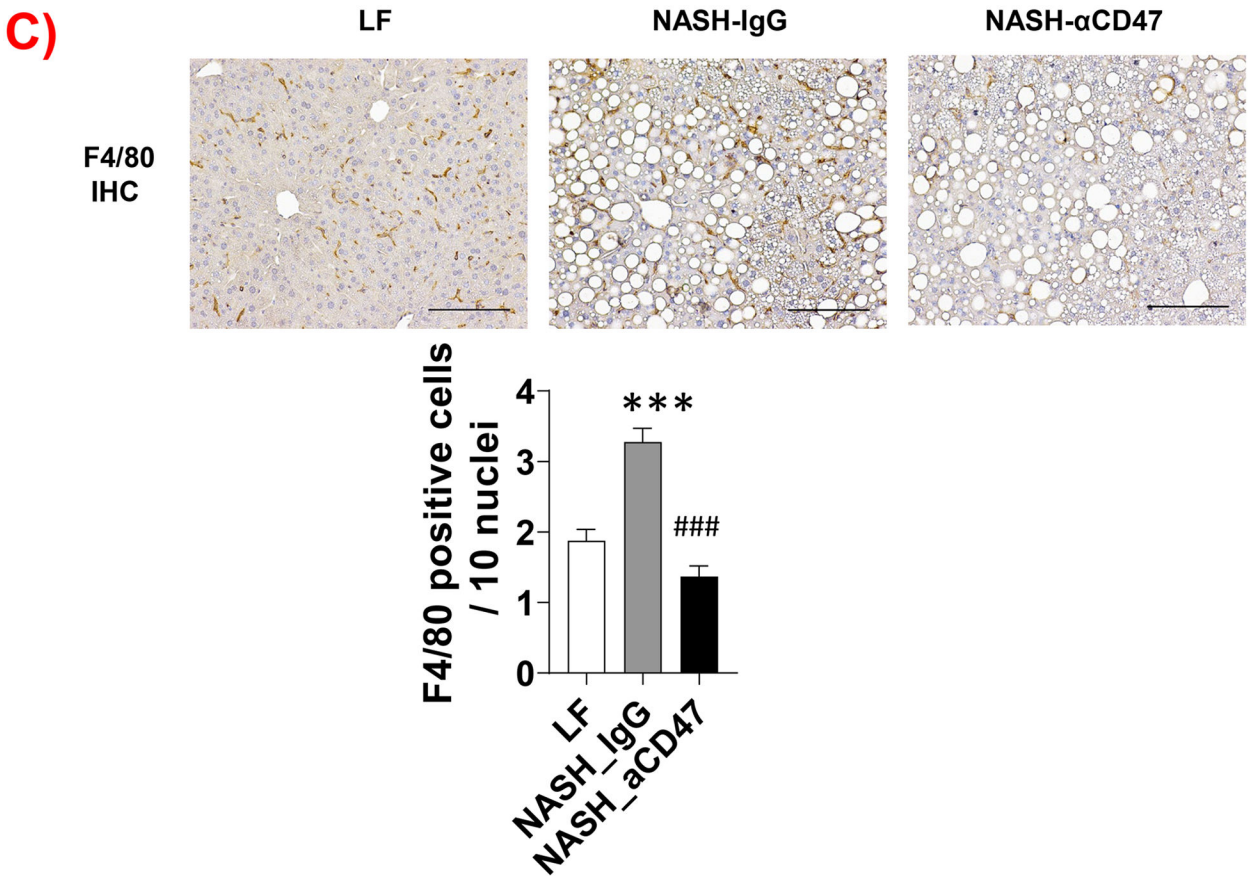

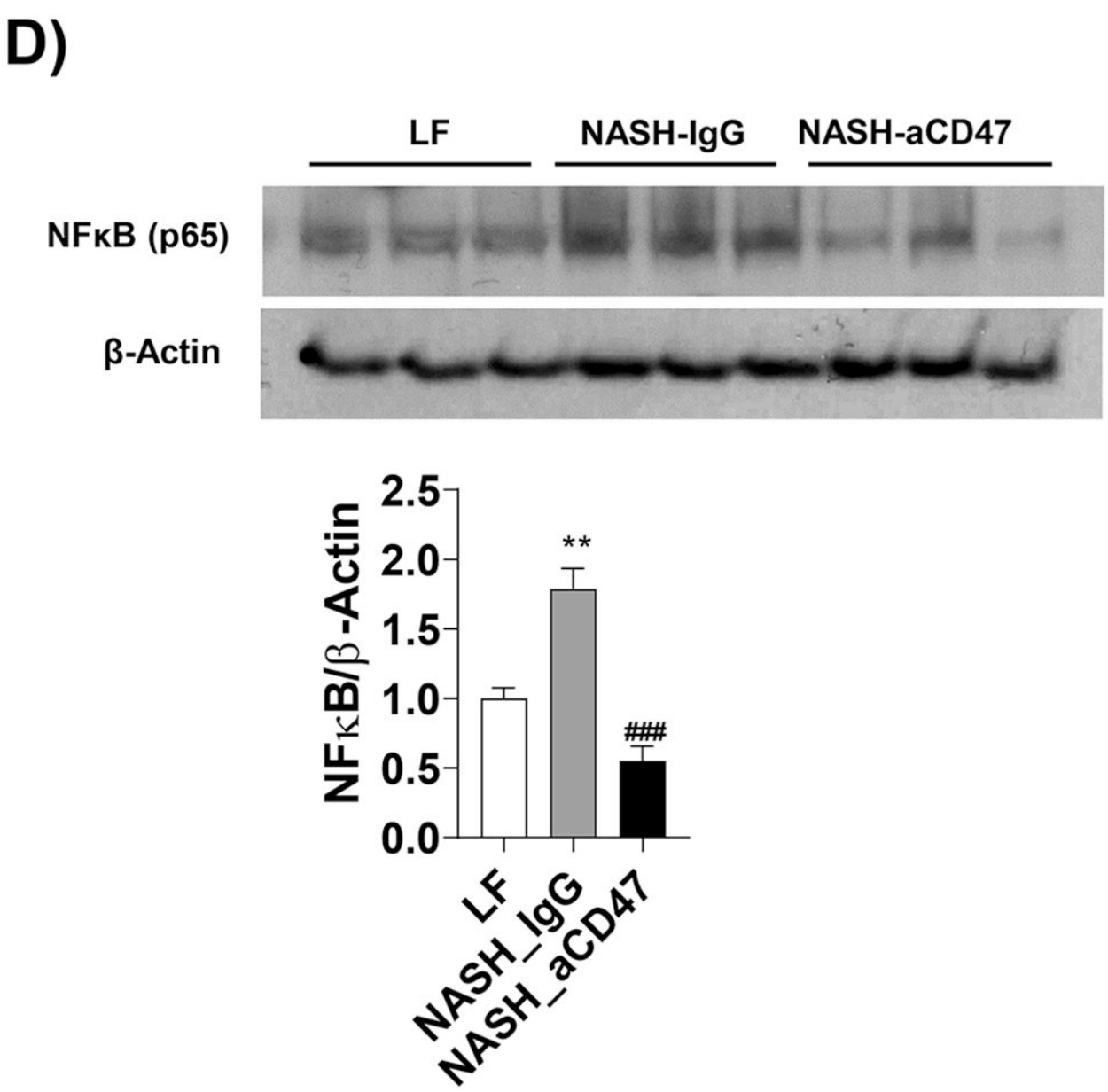

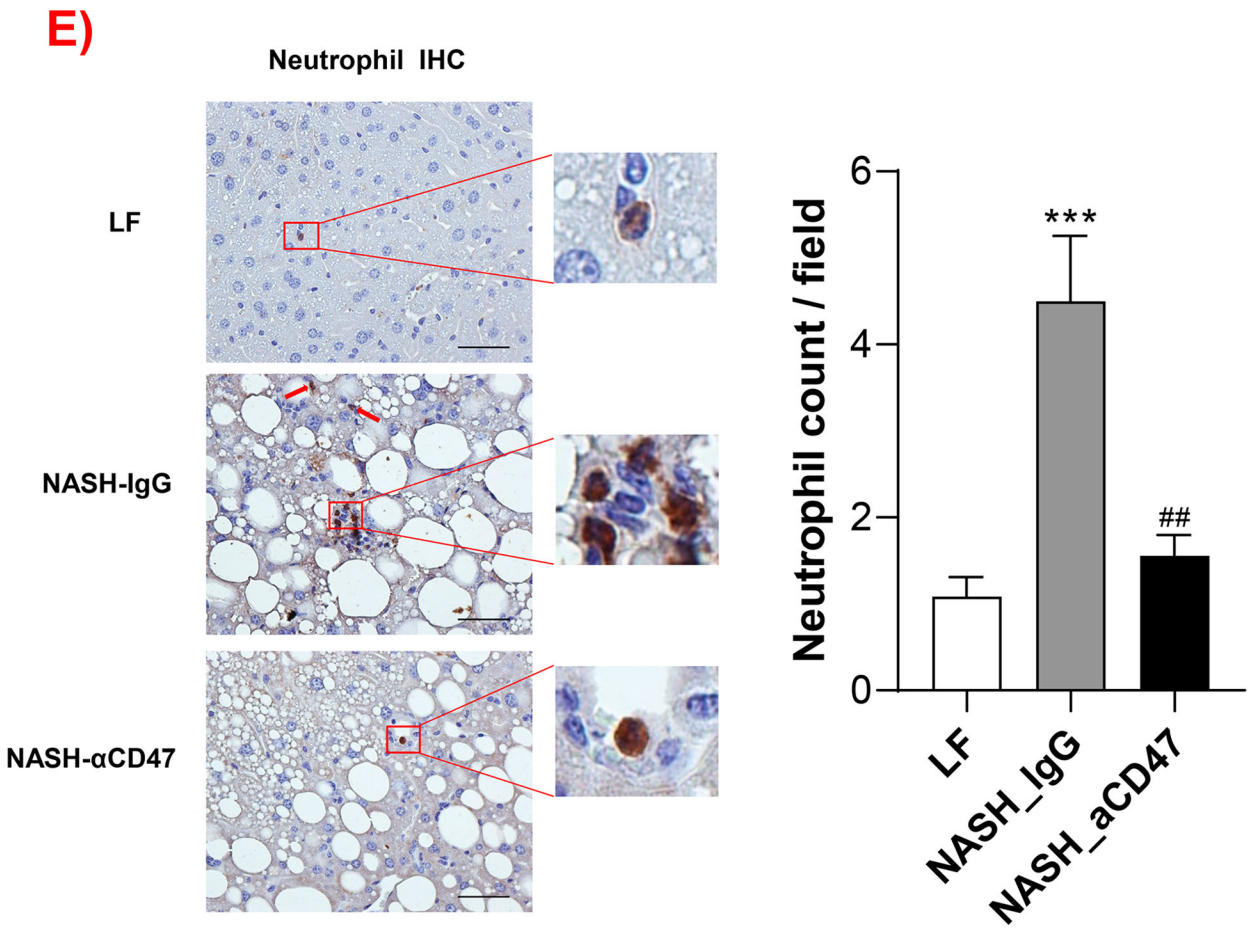

Fig. 3. Anti-CD47 antibody treatment attenuated AMLN diet-induced hepatic inflammation

(A) Hepatic inflammatory gene expression in liver by qPCR; (B) Representative liver immunofluorescent images (Blue=DAPI; Red=CD11b; Scale bar=100 μm) and the quantification data; (C) Representative liver immunohistochemical staining images for F4/80 (positive staining shown as brown color; Scale bar=100 μm) and the quantification data; (D). Western blotting and quantification of liver NF-κB/p65 levels normalized to β-actin levels. (E) Representative images for liver immunohistochemical staining of neutrophils from 3 groups of mice (positive staining shown as brown color, Scale bar=50 μm) and the quantification data. Data are represented as mean ± SEM (n=8 mice/group). **P*<0.05, ** *P*<0.01, and *** *P*<0.001 compared to LF; #*P*<0.05, ##*P* <0.01, and ###*P*<0.001 compared to NASH-IgG;

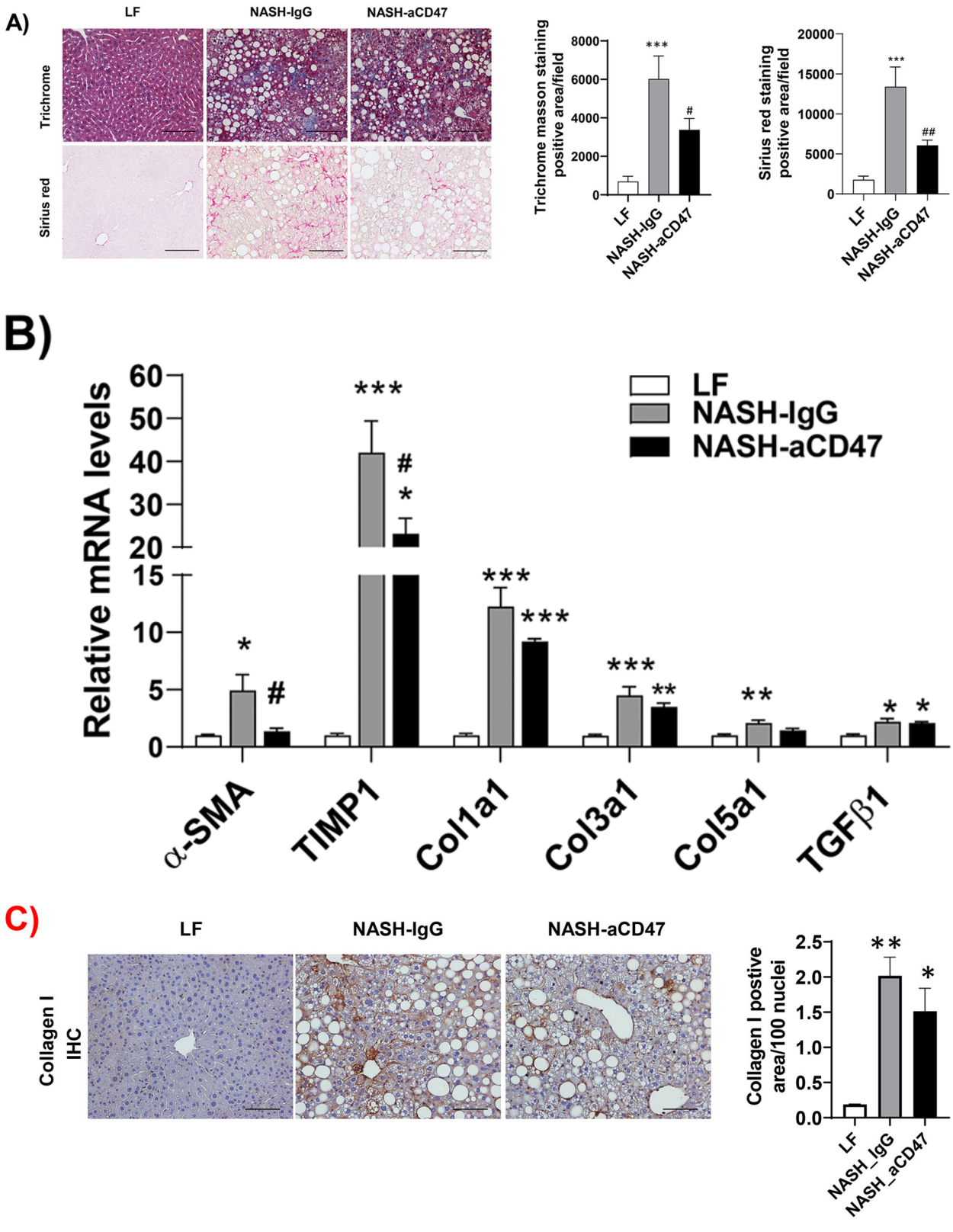

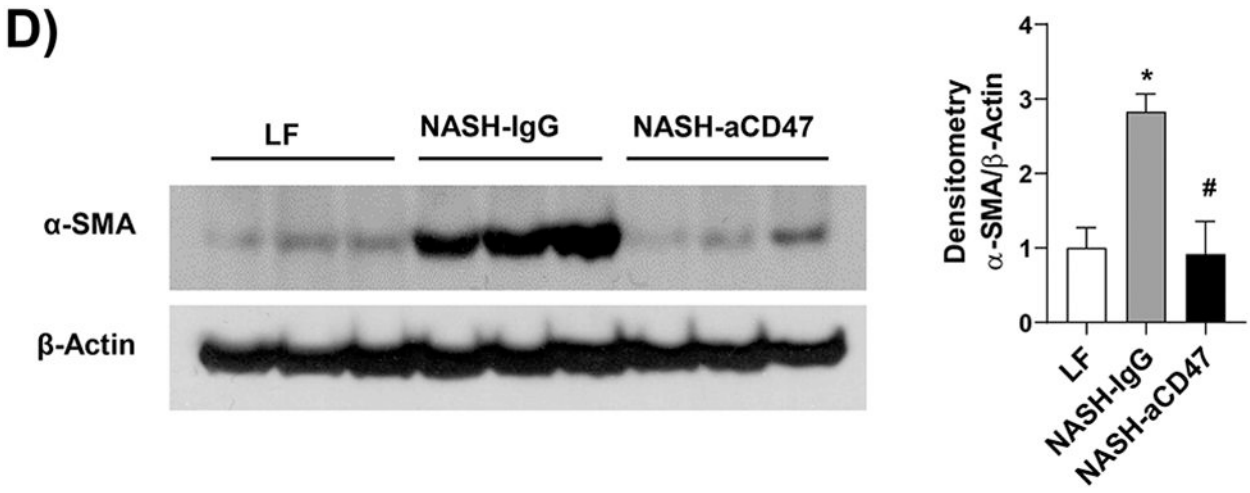

Fig. 4. Anti-CD47 antibody treatment attenuated AMLN-diet induced liver fibrosis

(A) Representative image of Trichrome staining (top panel) and Sirius red staining (bottom panel) and quantification of liver sections from 3 groups of mice (Scale bar=100 μm); (B) Hepatic fibrosis related gene expression in liver by qPCR; (C) Representative liver immunohistochemical staining images for Collagen I (positive staining shown as brown color; Scale bar=100 μm) and the quantification data; and (D) Western blotting and quantification of liver α-SMA levels from 3 groups. Data are represented as mean ± SEM (n=8 mice/group). **P*<0.05, ** *P*<0.01, and *** *P*<0.001 compared to LF; #*P*<0.05, ##*P*<0.01 compared to NASH-IgG

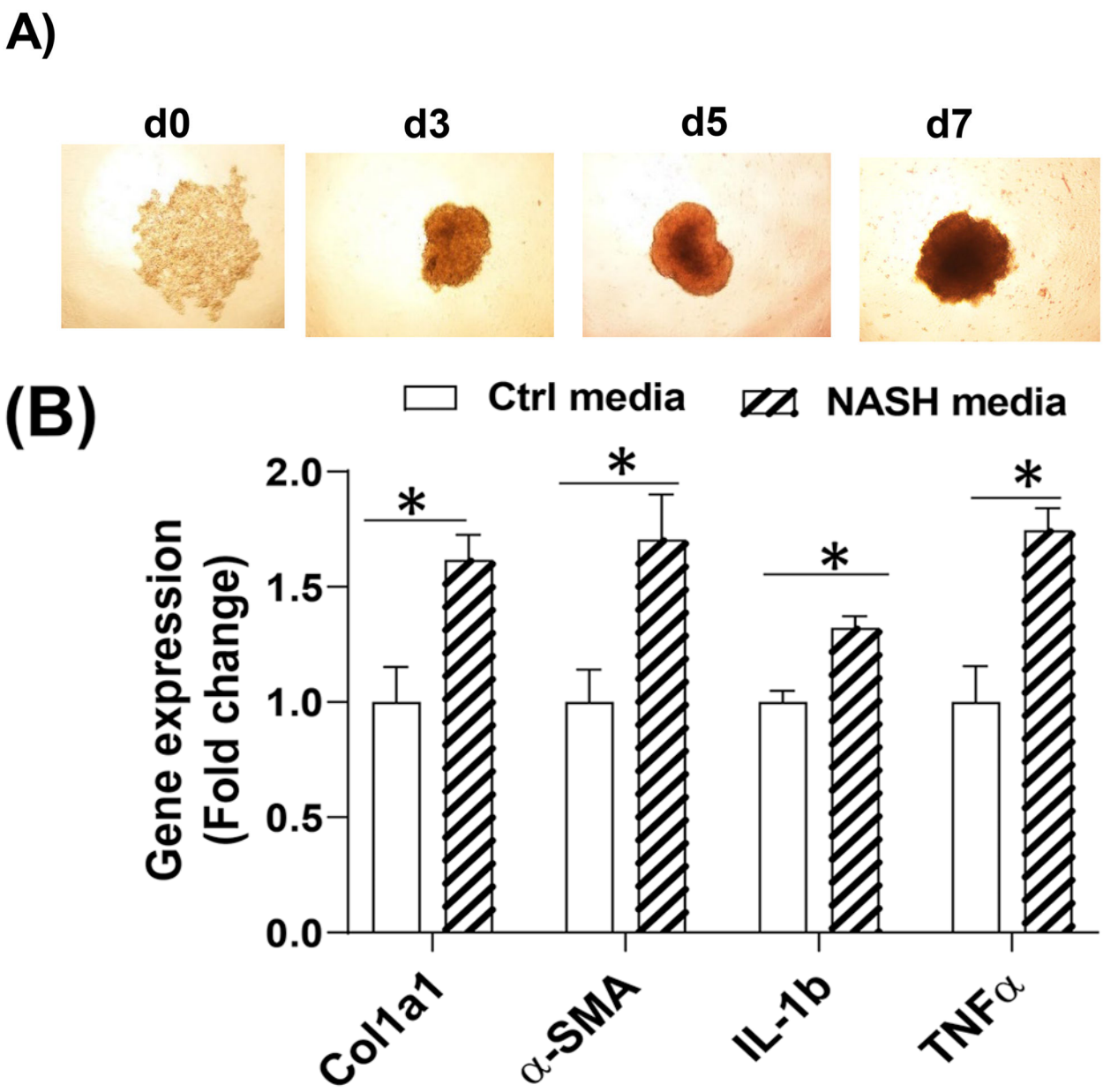

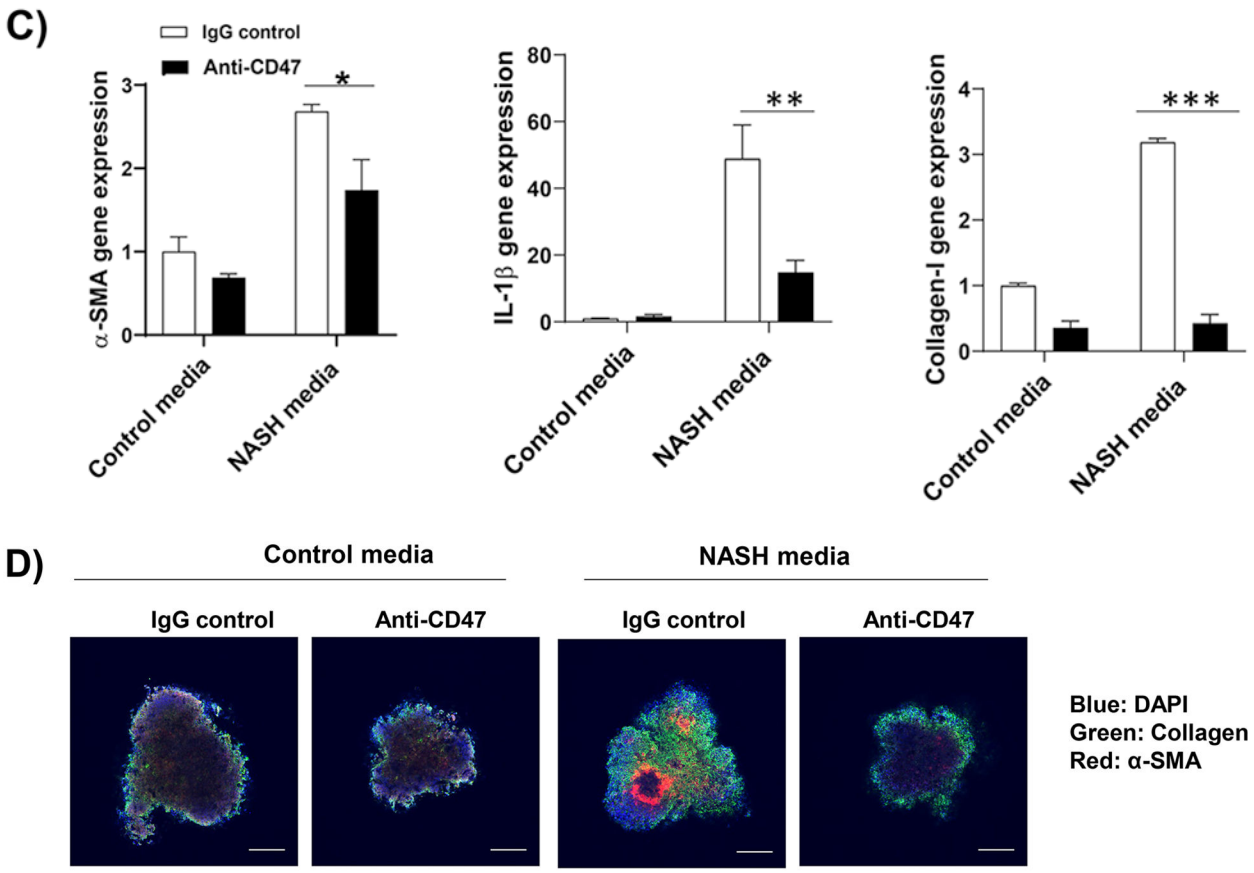

Figure 5: Anti-CD47 treatment attenuated liver inflammation and fibrosis in human NASH organoid

In vitro 3D human NASH model was established by co-culture of human hepatocyte/ THP-1-derived macrophages/human stellate cells to form spheroid. (A) Representative phase contrast images of 3D spheroid; (B) Spheroid was treated with NASH inducing media for 5 days to induce inflammation and fibrosis. Gene expression was determined by qPCR; (C) Spheroid was treated with NASH inducing media for 5 days and then treated for additional 5 days in the presence of control IgG or anti-CD47 antibody (20 μg/ml). Gene expression was determined by qPCR. Data are represented as mean ± SE (n=3 separate experiments). *P<0.05; **P<0.01; ***P<0.001; (D) Representative immunofluorescent images from human NASH organoid (Blue = DAPI; Green = Collagen I; Red = αSMA). Scale bar = 200 μm.

Table 1.

Blood profile

Parameters	LF	NASH-IgG	NASH-aCD47
WBC count (10^3/μl)	2.18±0.785	4.27±1.667 **	2.76±0.633 #
Neutrophil count (10^3/μl)	0.46±0.309	1.14±0.468 **	0.899±0.227
Lymphocytes count (10^3/μl)	1.65±0.582	2.92±1.389 *	1.74±0.371 #
Monocytes count (10^3/μl)	0.07±0.0475	0.15±0.144	0.08±0.033
Eosinophil count (10^3/μl)	0.01±0.000	0.1±0.0793	0.06±0.043
RBC (10^6/μl)	8.10±0.512	7.8±1.600	6.77±0.657 *
Hemoglobin (g/dL)	10.99±0.613	10.59±2.064	9.53±0.801
Hematocrit (%)	39.05±1.426	37.08±7.284	34.95±3.689
MCV (fL)	48.29±1.850	47.61±2.026	51.56±0.913 **
MCH (Pg)	13.6±0.680	13.59±0.658	14.09±0.387
MCHC (g/dL)	28.13±0.968	28.59±1.332	27.33±0.997
RDW (%)	17.6±1.077	18.78±0.466 *	17.61±0.846 #
Platelet (10^3/μl)	1071.25±128.694	1134.375±321.928	1281.75±148.780
MPV (fL)	4.762±0.177	4.16±0.278 ***	4.15±0.262 ***

Note:

* $P<0.05$

** $P<0.01$, and

*** $P<0.001$ compared to LF

# $P<0.05$ compared to NASH-IgG

Abbreviations: RBC: red blood cell; MCV: mean corpuscular volume; MCH: Mean corpuscular hemoglobin; MCHC: mean corpuscular hemoglobin concentration; RDW: red cell distribution width; MPV: mean platelet volume

Table 2.

Primer Sequences for QPCR

Gene	Primer sequence	Genes	Primer sequence
	Mouse primers		
FASN	5’-TCCTGGAACGAGAACACGATCT-3’ 5’-GAGACGTGTCACTCCTGGACTTG-3’	SCD-1	5’-TTCTTGCGATACACTCTGGTGC-3’ 5’-CGGGATTGAATGTTCTTGTCGT-3’
ACC	5’-CCCAGCAGAATAAAGCTACTTTGG-3’ 5’-TCCTTTTGTGCAACTAGGAACGT-3’	SREBP1c	5’-GGAGCCATGGATTGCACATT-3’ 5’-ACAAGGGTGCAGGTGTCACC-3’
HMGCS	5’-GACAAGAAGCCTGCTGCCATA-3’ 5’-CGGCTTCACAAACCACAGTCT-3’	HMGCR	5’-TGCACGGATCGTGAAGACA-3’ 5’-GTCTCTCCATCAGTTTCTGAACCA-3’
F4/80	5’-CTTTGGCTATGGGCTTCCAGTC-3’ 5’-GCAAGGAGGACAGAGTTTATCGTG-3’	CD11b	5’-CGGAAAGTAGTGAGAGAACTGTTTC-3’ 5’-TTATAATCCAAGGGATCACCGAATTT-3’
CD11c	5’-CTGGATAGCCTTTCTTCTGCTG-3’ 5’-GCACACTGTGTCCGAACTC-3’	MCP-1	5’-CAGCCAGATGCAGTTAACGC-3’ 5’-GCCTACTCATTGGGATCATCTTG-3’
IL-1β	5’-TGGAGAGTGTGGATCCCAAGCAAT-3’ 5’-TGTCCTGACCACTGTTGTTTCCCA-3’	TNFα	5’-AGCCGATGGGTTGTACCT-3’ 5’-TGAGTTGGTCCCCCTTCT-3’
TGFβ	5’-ACAATTCCTGGCGTTACC-3’ 5’-GGCTGATCCCGTTGATTT-3’	α-SMA	5’-ATTGTGCTGGACTCTGGAGATGGT-3’ 5’-TGAGTCACGGACAATCTCACGCT-3’
TIMP1	5’-TCTTGGTTCCCTGGCGTACTCT-3’ 5’-GTGAGTGTCACTCTCCAGTTTGC-3’	Col1a1	5’-TTCTCCTGGCAAAGACGGACTCAA-3’ 5’-AGGAAGCTGAAGTCATAACCGCCA-3’
Col3a1	5’-TCCTAACCAAGGCTGCAAGATGGA-3’ 5’-ATCTAGATCCCGCCCTTGGTTTGT-3’	Col5a1	5’-TCTCTGTGTGTGTGCCAAGATGGA-3’ 5’-AGCCAGAGTCCATCCCACATTTCT-3’
GAPDH	5’-AACTTTGGCATTGTGGAAGG-3’ 5’-GGATGCAGGGATGATGTTCT-3’		
	Human primers		
GFAP α-SMA	5’-GCAGAGATGATGGAGCTCAATGACC-3’ 5’-GTTTCATCCTGGAGCTTCTGCCTCA-3’ 5’-CCAGAGCCATTGTCACACAC-3’ 5’-CAGCCAAGCACTGTCAGG-3’	Col1a1	5’-GGATTCCAGTTCGAGTATGG-3’ 5’-CAGTGGTAGGTGATGTTCTG-3’
TNFα	5’-CACCACTTCGAAACCTGGGA-3’ 5’-AGGAAGGCCTAAGGTCCACT-3’	β-Actin	5’-CATGTACGTTGCTATCCAGGC -3’ 5’-CTCCTTAATGTCACGCACGAT -3’
IL-1β	5’-CAACAGGCTGCTCTGGGATT-3’ 5’-CATGGCCACAACAACTGACG-3’	CD68	5’-GCTACATGGCGGTGGAGTACAA-3’ 5’-ATGATGAGAGGCAGCAAGATGG-3’